ISSN: 0975 -8542

Journal of Global Pharma Technology

Available Online at: www.jgpt.co.in

RESEARCH ARTICLE

Synthesis, Identification, Theoretical and Experimental Studies for Carbon Steel Corrosion Inhibition in Sea Water for New Urea and Thiourea Derivatives linkage to 5-Nitro Isatin Moiety

Athraa Hikmat Ahmad[1], Rehab Majed Kubba[1], Suaad Mohammed Hussain Al-Majidi[1*]

Department of Chemistry, College of Science, University of Baghdad, Baghdad, Iraq.

***Corresponding Author: Suaad Mohammed Hussain Al-Majidi**

Abstract

This research includes synthesis of some new heterocyclic derivatives of 5-Nitroisatin namely 5-Nitro-3-(Ethyl imino acetate)-2-oxo indole (1), 5-Nitro-3-[(imino Aceto) urea]-2-oxo indole (2), 5-Nitro-3-[(imino Aceto)thiourea]-2-oxo indole (3), and 5-Nitro-3-[(imino Aceto) phenylthiourea]-2-oxo indole (4), and characterized by FTIR, ^{1}H-NMR and some physical properties. Theoretically, the inhibition efficiency parameters with physical properties were calculated to ensure for possibility using these compounds as inhibitors. Experimentally, studying the chosen compound of the corrosion inhibition efficiency for carbon steel in 3.5% NaCl solution by isatin derivative is chosen theoretically as the best inhibitor using potentiodynamic polarization.

Keywords: *Isatin derivatives, Schiff bases, Corrosion inhibitor, DFT quantum mechanical calculation.*

Introduction

Isatin (1H-indole-2, 3-Dione) consist of indole ring and two types of carbonyl groups i.e. keto and lactam group. It was first investigated by Erdman and Laurent [1] in 1841 as a product from the oxidation of indigo by nitric and chromic acid [2], Figure 1.

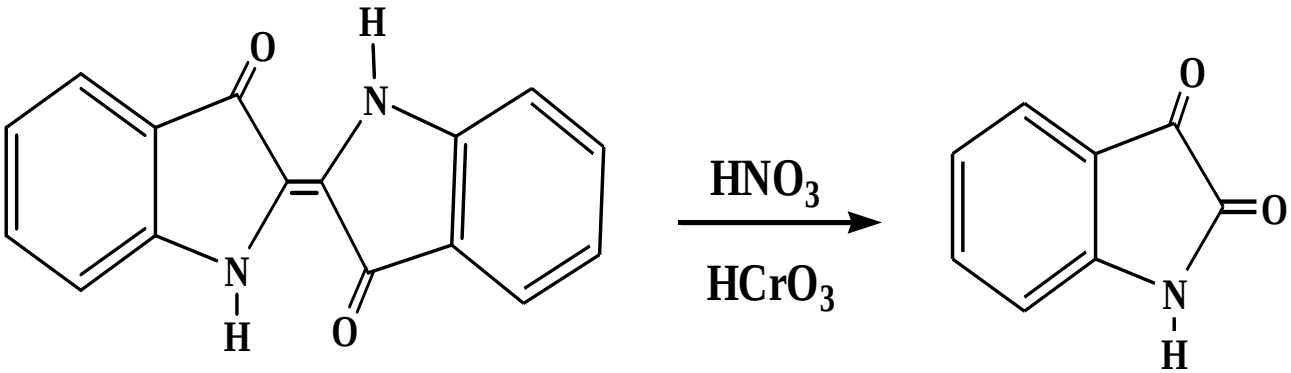

Figure 1

Schiff bases are usually synthesized from the condensation of primary amines and active carbonyl groups. They are one of the important compounds owing to their wide range of biological activities and industrial applications [3]. Some of Schiff bases were reported earlier as corrosion inhibitors for steel. These substances generally become effective as inhibitors by adsorption on the metal surface, for having -CH=N- imines group in the Schiff base molecules [4]. The quantum chemical calculations based on density functional theory (DFT) method; it

gives basic parameters for complex molecules [5].

Corrosion of metal surfaces [6] can be controlled by the addition of chemical compounds. This form of corrosion control is called inhibition and the compounds added are known as corrosion inhibitors. Generally, the heterogeneous organic compounds having higher basicity hetero atoms like O, N, and S have the tendency to resist corrosion [7].

The main objective of this investigation is to synthesize new 5-Nitro isatin derivatives and study the inhibitive effect for the mild steel corrosion in seawater, theoretically by using DFT method then experimentally by using potentiostatic methods.

Experimental Details

Synthesis of 5-Nitro Isatin Derivatives

Synthesis of 5-Nitro-3-(Ethyl imino acetate)-2-oxo indol (1) [8]

A mixture of 5-nitro isatin (2.5g, 0.0079mol), ethyl glycinate (1.054 g, 0.0079 mol) in absolute ethanol (10mL) with a few drops of glacial acetic acid was refluxed for (12) hrs. After that, the mixture was cooled to room temperature and precipitated.

The precipitate was poured into ice, filtered, dried and recrystallized from ethanol-water to give the product as red crystals .The physical properties in Table 1.

Synthesis of 5-Nitro-3-[(imino Aceto) urea]-2-oxo indole (2), 5-Nitro-3 [(imino Aceto) thiourea]-2-oxoindole (3) and 5-Nitro-3 [(imino Aceto) phenylthiourea]-2-oxoindole (4) [9]

In 50 ml round bottom flask, a mixture of (1 g, 0.0031 mol.) of compound **(1)** with (0.0031 mol) of [urea, thiourea, or phenyl thiourea respectively for preparing compounds **(2, 3 and 4)** respectively] and (0.25 g, 0.0031 mol) of sodium acetate in (8 ml) absolute ethanol, were refluxed for (10-12) hrs.

The mixture was poured into ice, filtered, dried and recrystallized from ethanol-water. The physical properties of compounds **(2-4**) are listed in Table 1.

Preparation of Solutions

Blank Solution

35 gm of NaCl was dissolved in distal water, transfer to a 1L volumetric flask, adding 2ml DMSO then complete the volume with distal water.

5-Nitro-3-[(imino Aceto) phenyl thiourea]-2-oxoindole (4) Solutions

Three concentrations of (5, 10 and 20 ppm) were prepared by dissolving (0.005, 0.01 and 0.02 gm), of compound **(4)**, in 2 ml DMSO, transfer to the volumetric flask of 1L. Then 35gm of NaCl was added to each concentration after dissolving in distal water before completing the volume to 1L.

Electrochemical Measurements

Potentiostatic Polarization Study

The potentiostat set up includes a Host computer, thermostat, magnetic stirrer, Mat lab (Germany, 2000), potentiostat, and galvanostat. The cell is (1L) capacity made of Pyrex consists of internal and external bowls. The electrochemical corrosion cell is three electrodes.

Carbon steel as a working electrode used to determine the potential of it according to the reference electrode, an auxiliary electrode is platinum with length (10cm) and reference electrode a silver-silver chloride (Ag/AgCl, 3.0M KCl).

The working electrode was immersed in the test solution for 30 minutes to establish steady state open circuit potential (E_{ocp}), then electrochemical measurements were performed in a potential range of (±200) mV. All tests were carried out at the temperature of (298-318K) controlled by using a cooling-heating circulating water bath.

Results and Discussion

Synthesis of 5-Nitro Isatin Derivatives

5-nitro isatin was reacted with ethyl glycinate, few drops of glacial acetic acid (HOAc) and absolute ethanol to give compound **(1),** which was used as a starting material for synthesis the **(2-4)** heterocyclic compounds by a reaction with nitrogen nucleophiles (e.g., urea, thiourea and phenylthiourea) in absolute ethanol to give compounds **(2-4)** respectively, as shown in Scheme 1.

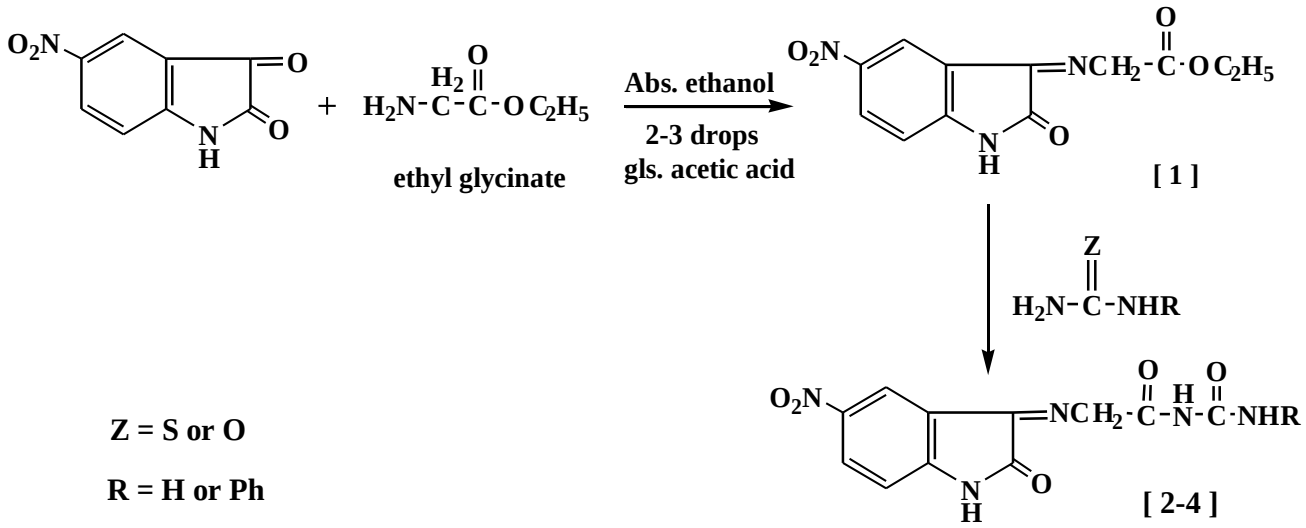

Scheme 1: Preparation of compounds (1-4)

The mechanism involved two steps: the first step is the condensation reaction between ethyl glycinate and carbonyl compounds, involving the nucleophilic addition of ethyl glycinate to carbonyl group producing an intermediate. The second step is the eliminating of water molecule [8], to afford the desirable Schiff's bases compound **(1)** as shown in Scheme 2.

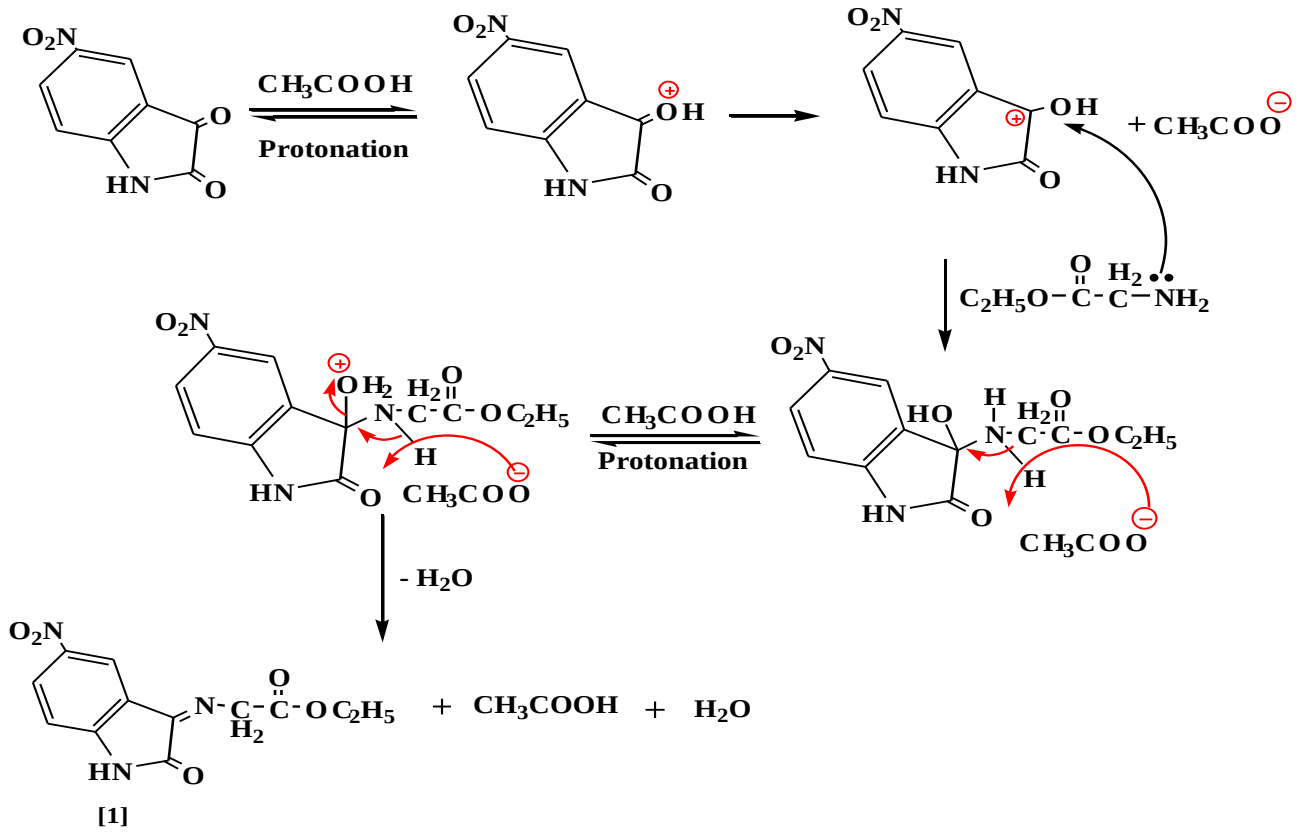

Scheme 2

The physical properties **(1)** are shown in Table 1. The FT-IR spectrum of compound **(1)** showed a new absorption bands (υ, cm^{-1}) appear at (2989, 2927) for (C-H) stretching aliphatic, 1735 for C=O stretching (ester overlap with amide); and 1627 for C=N imine group in addition to appearance of the characteristic absorption bands at (1255, 1191) for (C-O-C) bending vibration, Table 2.

The ^{1}H-NMR (DMSO-d_6) spectrum (δ, ppm) of compound (1) showed a signal at 1.3 (t, 3H, terminal CH_3), a quartet signal at 4.3 due to (-O-C$\underline{H}_2$), singlet signal at 4.91 due to (=N-C$\underline{H}_2$-), signal at 6.8 -8.5 (m, 3H, ArH), and signal at 11.1 for (-N$\underline{H}$), Table 3. The following mechanism described the formation of compounds (2-4) [8], Scheme 3.

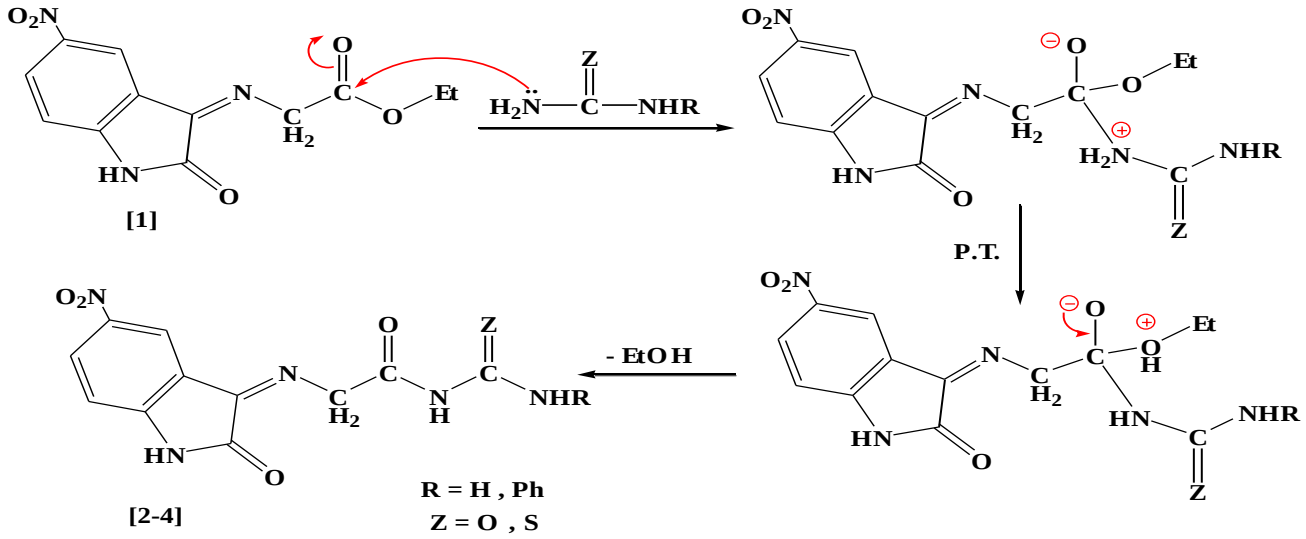

Scheme 3

The physical properties are shown in Table 1. The FT-IR spectrum for compound **(2)** showed absorption bands (υ, cm^{-1}) at (3442, 3353) for asymmetric and symmetric NH_2 stretching respectively, and 1681 for C=O amide. For compound **(3)**, the FTIR spectrum showed absorption bands at (3463, 3375) for asymmetric and symmetric stretching of NH_2, 3282 for NH and 1251 for C=S stretching. For compound **(4),** FTIR showed absorption bands at 1629 for C=N, 1230 for C=S, Table 2. The ^{1}H-NMR spectrum (δ, ppm) of compound **(2)** showed a signal at 4.3 for (=N-C$\underline{H_2}$-), multiple signals at 7.1-7.5 due to benzene ring protons, and a single signal at 8.09 due to (-N$\underline{H_2}$). ^{1}H-NMR spectrum (δ, ppm) of compound **(4)** showed signal bands at 4.3 (S, 2H, =N-C$\underline{H_2}$-); signal at 6.8-8 (m, 3H, ArH), signal at 9.1 (s, 1H, -NH-ph), signal at 11.1 for (-NH-) proton, and signal at 12 ppm due to (CO**NH**CS) proton, Table 3.

Table 1: Physical properties of compounds (1-4)

Comp No.	Structure	Molecular formula	M.W g/mol	m.p °C	Yield %	Color	Solvent of recryst.
1	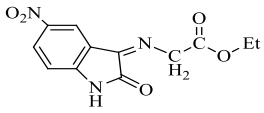	$C_{12}H_{11}N_3O_5$	277.23	160-165	70	Dark red	Ethanol-water
2	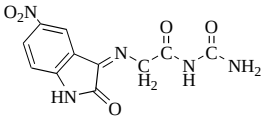	$C_{11}H_9N_5O_5$	291.22	148-150	85	Brown	Ethanol-water
3	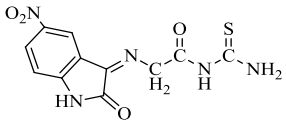	$C_{11}H_9N_5O_4S$	307.29	140-145	80	Brown	Ethanol-water
4	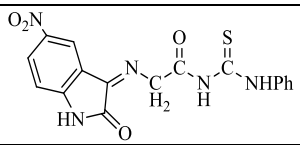	$C_{17}H_{13}N_5O_4S$	383.38	120-125	79	Brown	Ethanol-water

Table 2: FTIR spectral data (□, cm-1) of compounds (1-4)

Com. No.	Structure	ν(N-H)	ν(C-H) arom.	ν(C-H) aliph.	ν(C=O) Amide	ν(C=N)	Others
1	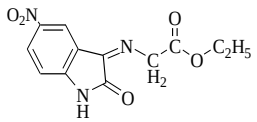	3330	3090	2989 2927	1735 Ester overlap with amide	1627	ν (C-O-C) Asym. 1255 Sym. 1191 ν (NO_2) Asym. 1514 Sym. 1330

2	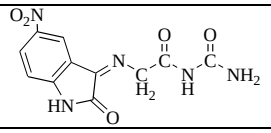	3261	3061	2920 2852	1681	1631	ν(NH_2) Asym. 3442 Sym. 3353
3	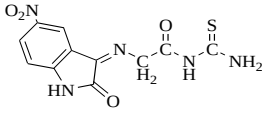	3282	3068	2908 2852	1697	1620	ν(NH_2) Asym. 3463 Sym. 3375 ν(C=S) 1251
4	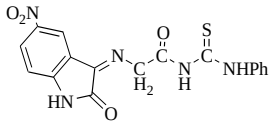	3336	3080	2985 2920	1703	1629	ν(NO_2) Asym. 1525 Sym. 1325 ν(C=S) 1230

Table 3: ^{1}H-NMR spectral data (δ, ppm) for compounds (1, 2, 4).

Comp. No.	Structure	^{1}H-NMR Spectral data (δ ppm)
1	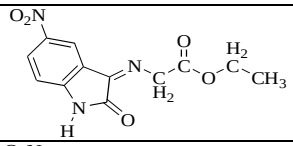	1.3 (t, 3H, C<u>H</u>$_3$); 4.3 (q, 2H, -OC<u>H</u>$_2$); 4.9 (s, 2H, =N-C<u>H</u>$_2$-); 6.8-8 (m, 3H, Ar-<u>H</u>); 11.1 (s, 1H,-NH).
2	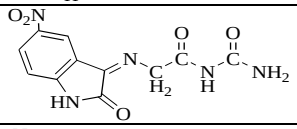	4.3 (s, 2H, =N-C<u>H</u>$_2$-); 7.1 -7.5 (m, 3H, Ar-<u>H</u>); 8.09 (s, 2H, NH_2) , 9.1 (s, 1H, -NH-); 11.0 (s, 1H, -NH)
4	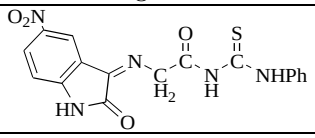	4.3 (s, 2H, =N-C<u>H</u>$_2$-); 6.8-8 (m, 3H, Ar-<u>H</u>); 9.1 (s, 1H, -NH-ph); 11.1 (s, 1H, -NH-); 12 (s, 1H, —C(=O)-N(H)-C(=S)—).

Theoretical Study

Quantum Chemical Calculations

The structural of the organic inhibitor and inhibition mechanism were carried out by using (DFT) Density Functional Theory utilizing Becke's three-parameter and the connection useful of Lee, Yang and Parr (B3LYP) together with the standard double-zeta plus polarization 6-311++G (2d, 2p) [10], for figuring the optimize geometries of the investigated molecules in vacuum and in three liquid media [ethanol (EtOH), dimethyl sulfoxide (DMSO) and water (H_2O)], all at the same level of DFT theory, Figure 2. This was implemented in the Gaussian 09 program package [11]. The parameters for the corrosion inhibition efficiency of the studied isatin derivatives were calculated at their equilibrium geometries, using (DFT) method. The optimized calculations for compounds **(1-4)** shown that they are all planner with Cs symmetry, and the order of the protection efficiency of the four investigated derivatives were determined according to the value of these parameters, which showed that compound **(4)** is the best with the order of **(4)> (3)> (2)> (1)**, and for all of these compounds, the calculated inhibition efficiency is increased in solvents more than in the vacuum, in the order of **(H_2O)> (DMSO)> (EtOH)> (vacuum)** Tables (4a, 4b)**.** So theoretically, compound **(4)** is expected to be the best as an inhibitor. So the complete information about this compound was studied and discussed theoretically such as (bonds length, bonds angles, electronic charges, and active adsorption sites etc).

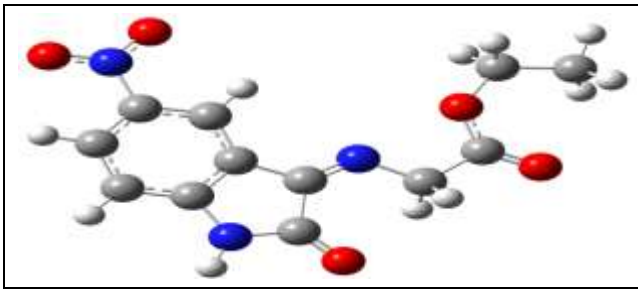

5-Nitro-3-(Ethyl imino acetate)-2-oxo indole (1).

5-nitro-3-[(imino aceto) urea]-2-oxo indole (2).

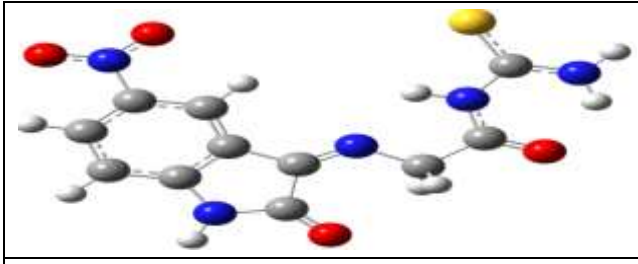

5-nitro-3-[(imino aceto) thiourea]-2-oxo indole (3).

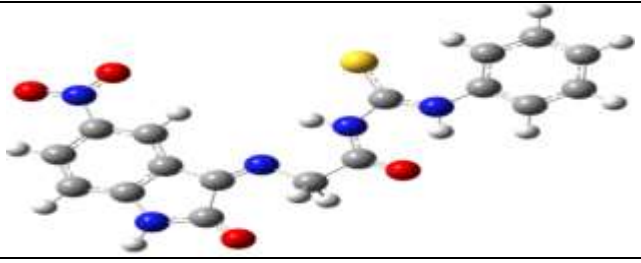

5-nitro-3-[(imino aceto) phenylthiourea]-2-oxo indole (4).

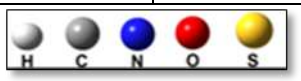

Figure 2: Equilibrium geometries of the studying 5-Nitro isatin derivatives (1-4) calculated by DFT (B3LYP/6-311++G (2d, 2p)) method

Table 4a: DFT calculated for some physical properties of the inhibitor molecules (1-4) at the equilibrium geometry

Inhib. medium	P. G.	M. formula	E_{HOMO} (eV)	E_{LUMO} (eV)	$\Delta E_{HOMO-LUMO}$ (eV)	μ (Debye)	E_{total} (eV)
(1)							
Vacuum	Cs	$C_{12}H_{11}N_3O_5$	-7.134	-3.244	3.890	3.4081	-27334.3
ETOH	Cs		-7.063	-3.103	3.960	5.0262	-27334.8
DMSO	Cs		-7.055	-3.101	3.954	5.0842	-27334.9
H_2O	Cs		-7.051	-3.100	3.951	5.1132	-27334.9
(2)							
Vacuum	Cs	$C_{11}H_9N_5O_5$	-7.587	-3.582	4.005	7.2242	-29246.6
ETOH	Cs		-7.121	-3.175	3.946	9.4041	-29247.4
DMSO	Cs		-7.107	-3.164	3.943	9.4784	-29247.3
H_2O	Cs		-7.101	-3.160	3.941	9.5130	-29247.3
(3)							
Vacuum	Cs	$C_{11}H_9N_5O_4S$	-6.138	-3.620	2.518	7.6253	-38034.7
ETOH	Cs		-6.575	-3.209	3.366	10.3398	-38035.4
DMSO	Cs		-6.590	-3.198	3.392	10.4353	-38035.5
H_2O	Cs		-6.597	-3.194	3.403	10.4798	-38035.5
(4)							
Vacuum	**Cs**	**$C_{17}H_{13}N_5O_4S$**	**-6.106**	**-3.658**	**2.448**	**7.6964**	**-44323.6**
ETOH	**Cs**		**-6.456**	**-3.240**	**3.216**	**10.3709**	**-44324.3**
DMSO	**Cs**		**-6.466**	**-3.231**	**3.235**	**10.4705**	**-44324.3**
H_2O	**Cs**		**-6.471**	**-3.226**	**3.245**	**10.5171**	**-44324.3**

Table 4b: Quantum chemical parameters for inhibitor molecules (1-4) as calculated using DFT method

Inhib. Medium	IP (eV)	EA (eV)	η (eV)	χ (eV)	S (eV)	ω (eV)	ΔN
(1)							
Vacuum	7.134	3.244	1.945	5.189	0.514	6.921	0.465
ETOH	7.063	3.103	1.980	5.083	0.505	6.524	0.484
DMSO	7.055	3.101	1.977	5.078	0.794	6.521	0.486
H_2O	7.051	3.100	1.975	5.075	0.506	6.520	0.487
(2)							
Vacuum	7.587	3.582	2.002	5.584	0.499	7.787	0.353
ETOH	7.121	3.175	1.973	5.148	0.506	6.716	0.469
DMSO	7.107	3.164	1.971	5.135	0.507	6.688	0.472
H_2O	7.101	3.160	1.970	5.130	0.508	6.679	0.474
(3)							
Vacuum	6.138	3.620	1.259	4.879	0.794	9.435	0.842
ETOH	6.575	3.209	1.683	4.892	0.594	7.109	0.626
DMSO	6.590	3.198	1.696	4.894	0.589	7.061	0.620
H_2O	6.597	3.194	1.701	4.895	0.587	7.042	0.618
(4)							
Vacuum	**6.106**	**3.658**	**1.224**	**4.882**	**0.816**	**9.735**	**0.865**
ETOH	**6.456**	**3.240**	**1.608**	**4.848**	**0.621**	**7.308**	**0.669**
DMSO	**6.466**	**3.231**	**1.617**	**4.848**	**0.618**	**7.266**	**0.665**
H_2O	**6.471**	**3.226**	**1.622**	**4.848**	**0.616**	**7.244**	**0.663**

Geometrical Optimization Structure for Compound (4)

The calculated optimize structure for compound **(4)**, representatives by the bond length, bond angles, and dihedral angles as shown in Table 5, according to the numbering of atoms shown in Figure 3.

The optimized geometrical structure was observed to be the same in the four media (vacuum, EtOH, DMSO, and H_2O).The compound under investigation shown that it is planar with symmetry of **Cs**, Figure 4. This result is confirmed by the values of dihedral angles [cis (0.0) and Trans (180.0)], Table 5.

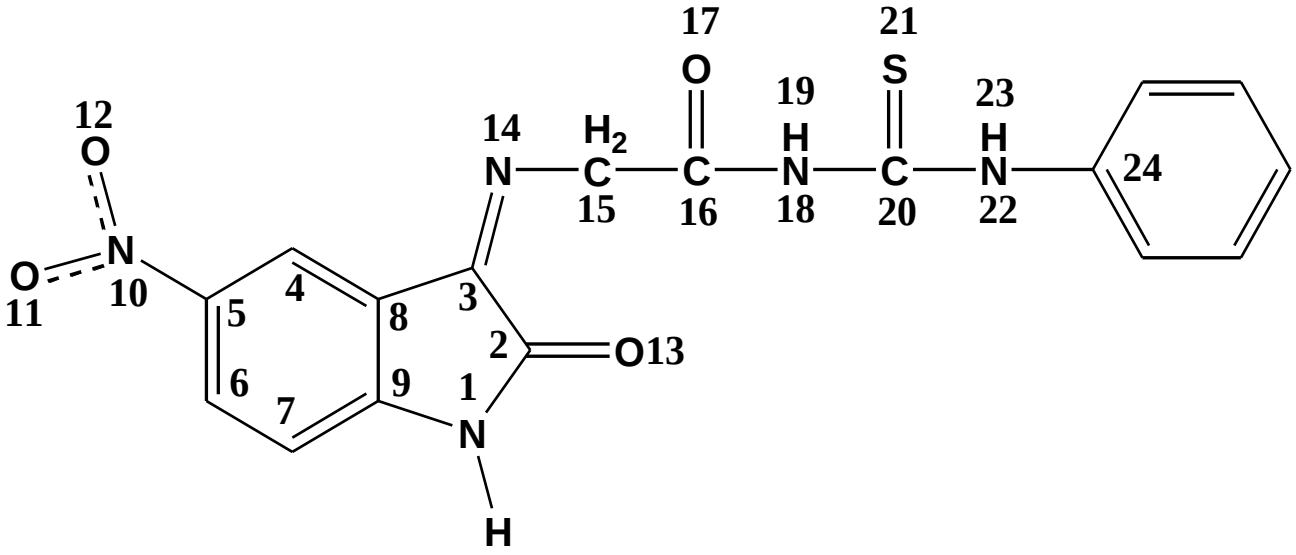

Figure 3: Labels for atoms of compound (4)

Table 5: Geometrical structure for compound (4) in the media of (vacuum, EtOH, DMSO, and H_2O) as calculated by using DFT method

Description bond length	Bond length (Å)	Description angle	Angle (deg)	Description dihedral angle	Dihedral angle (deg)
N1-C2	1.379	C2N1C9	111.840	N1C2C3C8	0.000
N1-C9	1.395	C2N1H	122.501	N1C2C3N13	180.000
C2-C3	1.525	N1C2C3	105.651	HN1C2O12	0.000
C2=O12	1.212	N1C2O12	126.340	C2C3C8C4	180.000
C3-C8	1.464	C2C3C8	105.502	C2C3C8C9	0.000
C3-N13	1.267	C2C3N13	127.786	C3C8C9C7	180.000
C4-C5	1.393	C6C5N10	118.606	C3C8C9N1	0.000
C4-C8	1.380	C5C6C7	120.274	C8C4C5C6	0.000
C5-N10	1.455	C3C8C9	107.472	C8C4C5N10	180.000
C6-C7	1.390	C3C8C4	131.928	C4C5C6C7	0.000
C7-C9	1.385	C7C9N1	128.641	N10C5C6C7	180.000
C8-C9	1.408	C5N10O11	117.889	C2C3N14C15	0.000
N10-O11	1.233	C3N14C15	121.083	C3N14C15C16	180.000
N14-C15	1.452	N14C15C16	112.567	N14C15C16O17	180.000
C15-H2	1.092	N14C15H2	111.531	N14C15C16N18	0.000
C15-C16	1.518	H2C15C16	107.778	O17C16N18C20	0.000
C16-O17	1.231	C15C16O17	119.219	C15C16N18C20	180.000
C16-N18	1.359	C16N18H19	115.716	C16N18C20S21	180.000
N18-C20	1.405	C16N18C20	129.972	N18C20N22C24	180.000
C20-S21	1.676	C18C20S21	116.089	S21C20N22C24	0.000
C20-N22	1.338	S21C20N22	130.012	.....	.....
N22-H23	1.021	C20N22C24	132.246	.....	.....
N22-C24	1.412	H23N22C24	114.798	.....	.....

Protection Efficiency Parameters for Compound (4)

Global Molecular Reactivity

Molecular Orbital Energies

The HOMO energy (E_{HOMO}) is often inhibitors with high values of E_{HOMO} have a tendency to donate electrons conversely, the LUMO energy (E_{LUMO}) indicates the lowest its value the higher accepting electrons. The gap energy between the Frontier orbital's ($\Delta E_{HOMO-LUMO}$) is an important factor in describing the molecular activity, so when the gap energy decreased, the inhibitor

efficiency is improved. The optimized structures of the studied compounds in the neutral form including their HOMO and LUMO distributions density are shown in Figure 4.

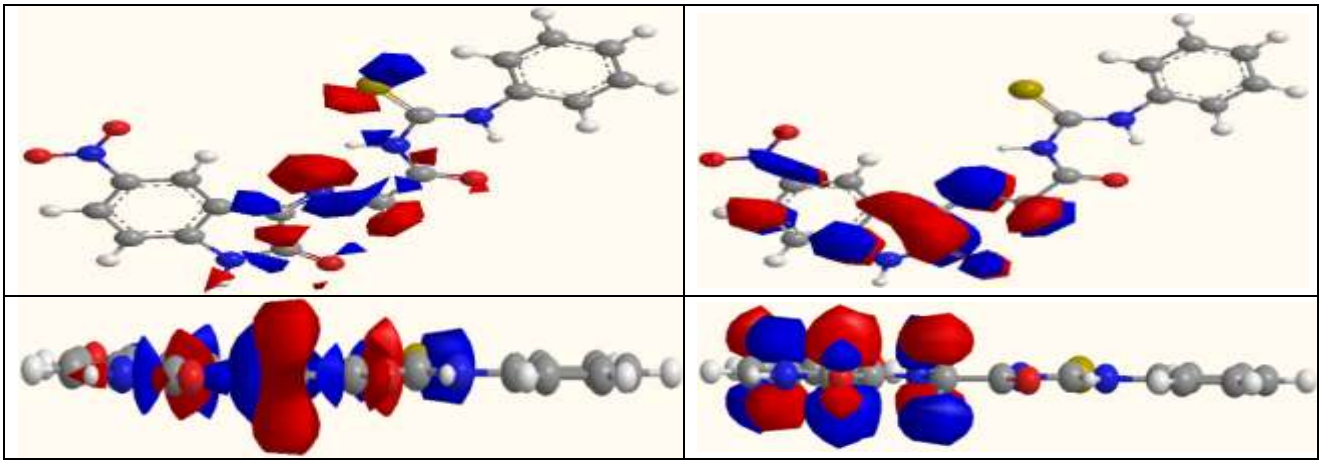

Figure 4: The Frontier molecule orbital density distributions of compound (4). [Red color: negatively charged lobe; blue color: positive charge lobe]

The E_{HOMO} for compound **(4),** in a vacuum, was (-6.106eV), decreased in EtOH, DMSO, and H_2O solvents. The (E_{LUMO}) in vacuum was (-3.658eV), also decreased in ETOH, DMSO and H_2O solvents and the value of $\Delta E_{HOMO-LUMO}$ were (2.448eV) in the vacuum, be a higher in EtOH (3.216eV), DMSO (3.235eV) and H_2O (3.245eV) Table 5. This indicates the increase in stability of the inhibitor in solvents in comparison with vacuum due to form the hydrogen bonding.

Dipole Moment

The dipole moment (μ in Debye) is the high value of dipole moment increases the adsorption of the inhibitor on a metal surface. The dipole moment for compound **(4)** in vacuum and EtOH, DMSO, H_2O are (7.696, 10.370, 10.470 and 10.517 Debye) respectively, Table 6.

Ionization Potential Energy (IE)

The ionization energy, **IE** can be expresed as the negative of the HOMO energy), Equation 1.

$$IE = -E_{HOMO} \quad (1)$$

So good inhibitors are of low energy of ionization .The IE of compound **(4)** inhibitor in the vacuum was (6.106eV), increased in the EtOH (6.456eV), DMSO (6.466eV) and H_2O (6.471eV), Table 7.

Electron Affinity (EA)

EA is the amount of energy released when adding an electron to an atom or molecule. The EA is associated with (E_{LUMO}) by the relation in Equation 2.

$$EA = -E_{LUMO} \quad (2)$$

A high value of EA means less stable inhibitor. Particles with high electron affinity realized as a good corrosion inhibitor.

The electron affinity of compound **(4)** in the vacuum is (3.658eV), be higher on using solvents of EtOH (3.240eV), DMSO (3.231eV) and H_2O (3.226eV), Table 7.

Chemical Hardness (η)

It is a measure of the ability of atom or molecule to transfer the charge. Increasing (η) decreases the stability of the molecule. It is calculated by using Equation 3:

$$\eta = (IE - EA)/ 2 \quad (3)$$

Compound possess a high value of (η) is considered to be a good inhibitor. The value of (η) for compound **(4)** in the vacuum was (1.224eV), be lower in EtOH (1.608eV), DMSO (1.617eV) and H_2O (1.622eV), Table 7.

Chemical Softness (S)

The measure of flexibility of an atom to receive electrons **(S)** was calculated using Equation 4:

$$S = 1/ \eta \quad (4)$$

Molecules of the high value of S are considered to be a good inhibitor. The value of (S) in the vacuum is (0.816eV), decreased

in ETOH, DMSO and H_2O to (0.621, 0.618, and 0.616eV) respectively, Table 7.

The Electro Negativity (χ)

The ability of an atom or a group to pull electrons (**χ**) can be calculated by using equation 5:

$$\chi = (IE+EA)/ 2 \quad (5)$$

Molecules of high electro negativity indicate to be good inhibitors. The calculated (**χ**) for compound **(4)** in the vacuum was found to be (4.882eV), decreased in solvents to be (4.848eV), Table 7.

Global Electrophilicity Index (ω)

ω is the measure of the stability of atom after gaining an electron. Good inhibition compounds are of a low value of (**ω**) which is calculated by using Equation 6.

$$\omega = \chi^2/ 2\eta \quad (6)$$

The values of (**ω**) are shown in Table 7. In the vacuum was (9.735eV), decreased in EtOH (7.308eV), DMSO (7.266eV) and H_2O (7.244eV) solutions.

ΔN (Difference in Number of Electrons Transferred)

The fraction of electrons transferred for an inhibitor to carbon steel surface was also calculated using theoretical values of χ_{Fe} and η_{Fe} for mild steel (7.0eVmol^{-1} and 0.0eV mol^{-1}) respectively.

The ΔN values are correlated to the inhibition efficiency resulting from electron donation .According to Lukovits et al. [12] if ΔN< 3.6, the inhibition efficiency increases with increasing electron-donating ability at the metal surface.

Table 7, according to DFT calculations; shows that the highest value of ΔN in the vacuum and solvent was related to compound (4) by the tendency of it to receive electrons from the metallic surface to unoccupied orbital (3d) of S atoms. This ability increases the inhibition efficiency. When two systems, Fe, and inhibitor, are brought together, electrons will flow from lower χ(inhibitor) to higher χ_{Fe}, until the chemical potentials become equal. The number of transferred electrons (**ΔN**) was calculated by using Equation 7.

$$\Delta N = \chi_{Fe} - \chi_{inhib} / [2\,\eta_{Fe} + \eta_{inhib.}] \quad (7)$$

Table 6: DFT calculations of some physical properties for compound (4) at the equilibrium geometry in the media of (vacuum, ETOH, DMSO, and H_2O)

Inhibitor medium	Sym.	E_{HOMO} (eV)	E_{LUMO} (eV)	$\Delta E_{HOMO-LUMO}$ (eV)	μ (Debye)	E_{total} (eV)
Vacuum	Cs	-6.106	-3.658	2.448	7.696	-1628.826
ETOH	Cs	-6.456	-3.240	3.216	10.370	-1628.851
DMSO	Cs	-6.466	-3.231	3.235	10.470	-1628.852
H_2O	Cs	-6.471	-3.226	3.245	10.517	-1628.852

Table 7: Quantum chemical parameters for compound (4) in the media of (vacuum, ETOH, DMSO, and H_2O)

Inhibitor medium	IE (eV)	EA (eV)	H (eV)	S (eV)	χ (eV)	ω (eV)	ΔN
Vacuum	6.106	3.658	1.224	0.816	4.882	9.735	0.865
ETOH	6.456	3.240	1.608	0.621	4.848	7.308	0.669
DMSO	6.466	3.231	1.617	0.618	4.848	7.266	0.665
H_2O	6.471	3.226	1.622	0.616	4.848	7.244	0.663

Local Reactivity of the one 5-nitro isatin Derivatives

The local of reactivity of the calculated compound is investigated through of the reactive centers of molecules (nucleophilic and electrophilic centers) using the DFT Mulliken charges population analysis. The molecule regions where the electronic charge is large are chemically softer than the regions where the electronic charge is small, so the electron density plays an important role in calculating the chemical reactivity.

Chemical adsorption interactions are either by orbital interactions or electrostatic. Electrical charges in the molecule considered

driving force of electrostatic interactions. Proven charges are important in physic-chemical properties of compound reactions [13]. Table 8 shows the order of the negative active sites for adsorption (nucleophilic reactive sites) as **N14< O13< O17< S21**, and the order of the positive active sites for adsorption (electrophilic reactive sites) as **C3< C2< C8< C20**.

Table 8: DFT Mulliken charges population analysis for the calculated inhibitor molecule compound (4) in media (vacuum, ETOH, DMSO, and H_2O)

Atom No.	Electronic charge/ ecu	Atom No.	Electronic charge/ecu	Atom No.	Electronic charge/ecu	Atom No.	Electronic charge/ecu
C1	-0.238V -0.224E -0.223D -0.223W	C7	**-0.300V** **-0.320E** **-0.321D** **-0.321W**	O13	**-0.450V** **-0.509E** **-0.511D** **-0.512W**	H19	**0.308V** **0.313E** **0.313D** **0.313W**
C2	**0.389V** **0.438E** **0.440D** **0.441W**	C8	**0.635V** **0.672E** **0.673D** **0.674W**	N14	**-0.195V** **-0.203E** **-0.203D** **-0.203**W	C20	**0.743V** **0.741E** **0.741D** **0.741W**
C3	**0.277V** **0.306E** **0.309D** **0.306W**	C9	**-0.269V** **-0.299E** **-0.300D** **-0.30**1W	C15	0.257V 0.242E 0.242D 0.241W	S21	**-0.688V** **-0.738E** **-0.740D** **-0.741W**
C4	-0.575V -0.548E -0.547D -0.547W	N10	**0.006V** **0.061E** **0.063D** **0.064W**	C16	-0.043V -0.001E -0.003D -0.004W	N22	**-0.105V** **-0.107E** **-0.107D** **-0.107W**
C5	-0.025V -0.020E -0.021D -0.021W	O11	**-0.154V** **-0.208E** **-0.210D** **-0.211W**	O17	**-0.471V** **-0.520E** **-0.522D** **-0.522W**	H23	**0.270V** **0.282E** **0.282D** **0.282W**
C6	**0.072V** **0.093E** **0.093D** **0.009W**	O12	**-0.118V** **-0.186E** **-0.189D** **-0.190W**	N18	-0.226V -0.213E -0.212D -0.211W	C24	-0.343V -0.282E -0.279D -0.278W

V: vacuum, E: ethanol, D: dimethyl sulfoxide (DMSO), W: water, blue color: increase in electronic charge to more positive, red color: increase in electronic charge to more negative

Corrosion Measurement of Compound (4)

Potentiostatic Polarisation Measurements

The electrochemical kinetics of metallic corrosion process can be characterized by determining at least three polarisation parameters, such as corrosion current density (I_{corr}), corrosion potential (E_{corr}) and Tafel slopes (ba and bc) listed in Table 9. [14].

However, a requirement for this method to be used is the graph of E versus log I must have at least one straight line [15].

Moreover, for an accurate evaluation of I_{corr}. By Tafel method, the linear regions should extend over about one decade on the log I_{corr} Axis [16]. The error in the numerical values of Tafel slopes can reduce the accuracy of the values calculated for I_{corr} [17]. Potentiodynamic polarisation curves for carbon steel in 3.5% NaCl at (298, 308, 318) K in the absence and in the presence of different concentration of compound **(4)** are shown in Figure 5.

The effect of increasing concentration and temperature on E_{corr}, I_{corr}, and Tafel slopes (bc and ba) are shown in Table, as well as protection efficiency PE%, and surface coverage Θ, which were calculated by using the following equations:

$$\%PE = (I_o - I)/ I_0 \times 100 \quad (8)$$

Where I_o and I: the corrosion current densities in the absence and presence inhibitor, respectively.

$$\Theta = \% PE / 100 \quad (9)$$

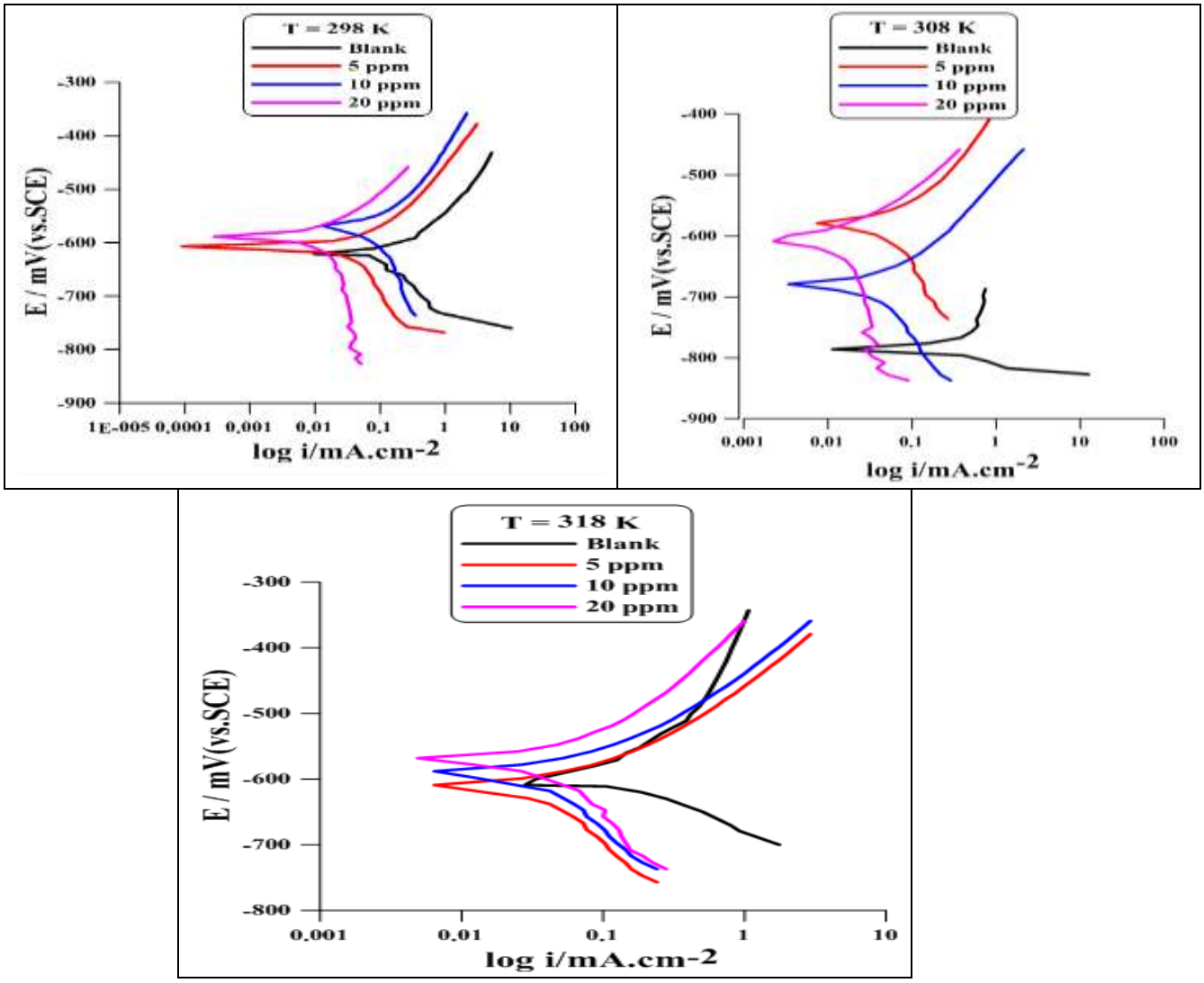

Figure 5: polarization plots of 3.5% NaCl carbon steel for blank and for various concentrations of compound (4) at the temperature (293, 308 and 318) K

Table 9: Corrosion data of carbon steel in 3.5% NaCl in absence and presence of various concentrations at a temperature of 298-318K

Inhib. conc. /ppm	T/K	E_{corr} (mV)	I_{corr} (µA.cm^{-2})	b_c (mV.dec^{-1})	b_a (mV.dec^{-1})	IE%	Θ
0	298	-621.0	121.69	-146.9	82.1	---	---
	308	-785.7	164.53	-26.3	73.8	---	---
	318	-608.0	191.16	-102.0	315.2	---	---
5	298	-607.60	17.37	-84.8	56.9	85.726	0.857
	308	-583.00	27.37	---	77.2	83.365	0.834
	318	-610.60	35.51	-191.5	82.5	81.424	0.814
10	298	-560.30	13.71	-106.1	68.7	88.733	0.887
	308	-576.80	22.05	-121.1	68.3	86.598	0.865
	318	-567.60	30.17	-152.6	88.3	84.217	0.842
20	298	-588.10	5.62	-97.5	59.8	95.381	0.953
	308	-608.10	8.83	-138.3	77.0	94.633	0.946
	318	-616.80	16.79	-180.1	72.9	91.216	0.912

Adsorption Isotherm Behavior

Adsorption isotherms describe the role of the inhibitors and contribute information about their interplay with the metal surface. These isotherms require the degree of surface coverage (Θ) for different inhibitor concentrations, which is calculated according to Equation 9. The adsorption behavior of compound (4) was found to obey Langmuir isotherms .The Langmuir adsorption isotherm, given by Equation 10.

$$C_{inh} / \Theta = 1/ K_{ads} + C_{inh} \quad (10)$$

Where, $C_{inh.}$ is the inhibitor concentration (mol. L^{-1}), $K_{ads.}$ is the adsorption/desorption equilibrium constant (L. mol^{-1}). The plot of ($C_{inh./} \Theta$) versus $C_{inh.}$ gave a straight line and the intercept represents (1/ $K_{ads.}$) with a slight deviation of the slope from unity as shown in the correlation coefficient values, Figure 6. $K_{ads.}$ is related to the standard Gibbs free energy of adsorption ($\Delta G_{ads.}$), Equation 11.

$$\Delta G_{ads.} = -2.303\ RT\ [\log 55.5 K_{ads.}] \quad (11)$$

Where R is the gas constant 8.314 $J.mol^{-1}.K^{-1}$, T is the temperature (K), and 55.5 is the molar concentration of water (mol. L^{-1}).

The free energy of adsorption ($\Delta G_{ads.}$) was calculated from Equation 12.

$$\Delta G_{ads.} = \Delta H_{ads.} - T\Delta S_{ads} \quad (12)$$

Where $\Delta H_{ads.}$, $\Delta S_{ads.}$ Are the change in enthalpy and entropy of adsorption respectively, calculated from plotting Log $K_{ads.}$ Versus (1/ T), Equation 13.

Equations 11 and 12 are combined to obtain Equation 13.

$$\text{Log } K_{ads.} = -\Delta H_{ads} / 2.303RT + \Delta S_{ads} / 2.303R + \text{Log } 1 / 55.5 \quad (13)$$

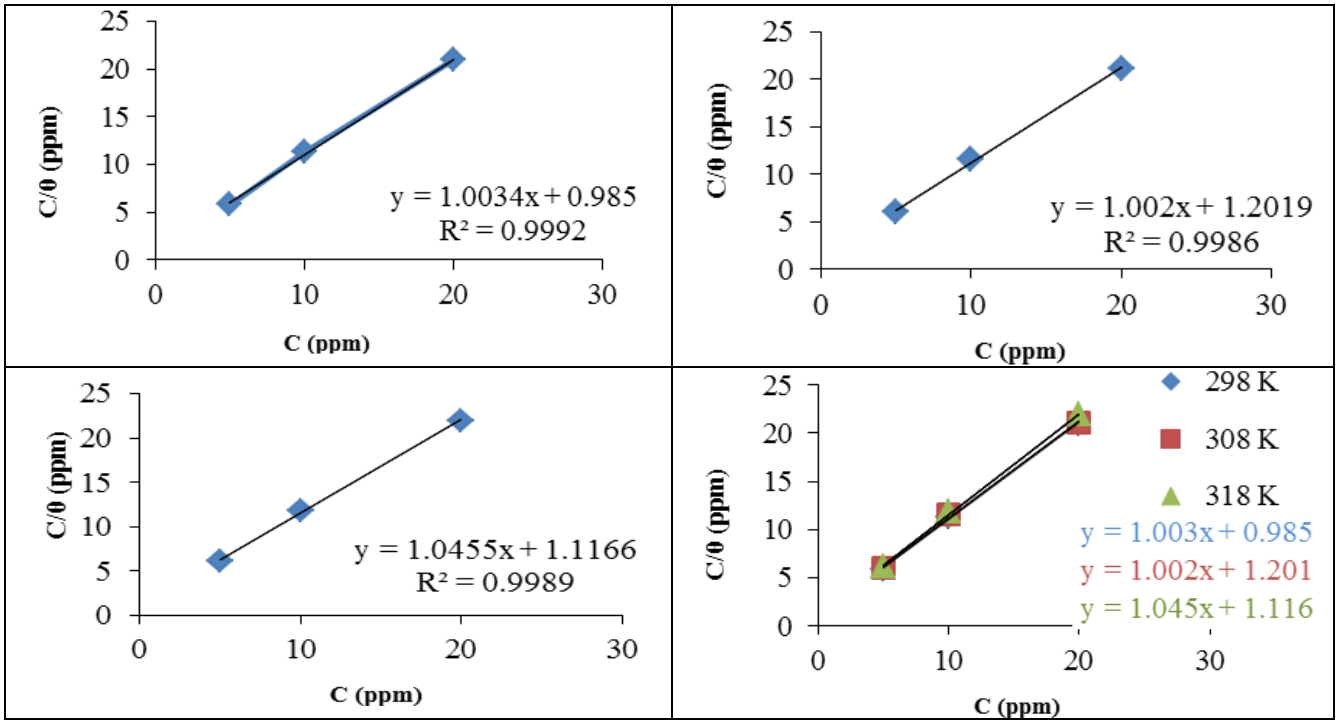

Figure 6: Langmuir isotherm plots for the adsorption of compound (4) on carbon steel at the temperatures range of (298-318)

The high values of $K_{ads.}$ Mean a strong interplay of compound **(4)** with the carbon steel surface in 3.5% NaCl, the optimum inhibition temperature is 298K, Table 10. The heterogeneous surface properties (i.e. flaws, impurities, cracks, and vacancies) of the steel are responsible for the differential $\Delta G_{ads.}$ Values obtained for compound **(4)** as the surface coverage value changes [18].The negative values of $\Delta G_{ads.}$ ensure the tendency of the adsorption process and stability of the adsorbed layer on the C-steel surface [19]. Moreover, it is found that $\Delta G_{ads.}$ is slight decreases in temperature. Generally, the values of the ΔG_{ads} negative sign are usually characteristic of a strong interaction. Generally, values of $\Delta G_{ads.}$ around -20 kJ mol^{-1} or lower negative are the electrostatic interaction between the molecules and the metal (physisorption). Whereas, the more negative values than -40 kJ mol^{-1} involve charge sharing to form a coordinate type of bond (chemisorption). Calculated ΔG_{ads} values indicate that the adsorption

mechanism of the synthesized inhibitor on carbon steel in 3.5% NaCl solution is physical adsorption [20].In the present study, the value of $\Delta G_{ads.}$ is of -9.99 to -9.68 kJ. mol^{-1}. Figure 6 shows the plotting of $C_{inh.}/\Theta$ versus $C_{inh.}$, a straight line were obtained, the adsorption of the compound **(4)** takes the Langmuir adsorption isotherm The thermodynamic parameters got ΔHads from slope and. the intercept represents ΔS_{ads}, Figure 7.A low value of $\Delta H_{ads.}$ shows an increase in the stability of the adsorbent inhibitor. $\Delta H_{ads.}$ of the negative value means exothermic adsorption process. Generally, an exothermic process purports either physisorption or chemisorptions while an endothermic process is attributable unequivocally to chemisorptions [21], Table 10. $\Delta S_{ads.}$ refers to random interaction**(4)**. Corrosion inhibition of C-steel in 3.5% NaCl solution by compound **(4)** can be explained on the basis of molecular adsorption. It is a mixed complex type comprehensive adsorption. This assuming is confirmed by data obtained for the temperature dependence of the inhibition process [22] and value of $\Delta G_{ads.}$

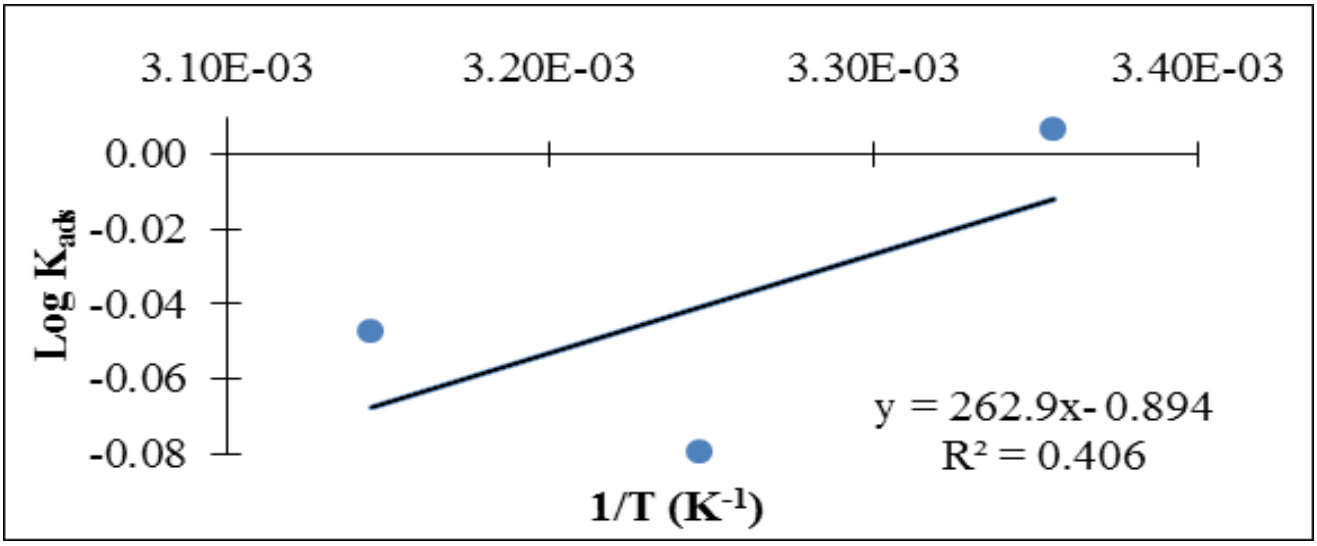

Figure 7: Plot of log $K_{ads.}$ vs (1/T) for compound (4)

Table 10: Thermodynamic parameters for adsorption of compound (4) on C-steel surface in 3.5% NaCl at different temperatures

T/K	K_{ads}	ΔG KJ. mol^{-1}	R^2	ΔH_{ads} kJ. mol^{-1}	ΔS_{ads} J. mol^{-1}.K
298	1.015228	-9.99235	0.999	-5.03378	0.2016003
308	0.832639	-9.50104	0.998		
318	0.896057	-9.68294	0.998		

Corrosion Kinetic and Thermodynamic Activation Parameters

Activation parameters were calculated for blank and different concentration (5, 10, 20 mL/L) of compound (4). To decide the activation vitality of the corrosion prosses, activation parameters are taken at different temperatures (298, 308, 318) K in the blank and different concentrations of compound (4). For calculating the activation parameters, Table 11, Arrhenius and Arrhenius transition state equations (14, 15) were used respectively.

$$\text{Log } (I_{corr}) = \text{Log } A - Ea/2.303RT \quad (14)$$

$$\text{Log } (I_{corr}/T) = \text{Log } (R/Nh) + \Delta S^*/2.303R - \Delta H^*/2.303RT \quad (15)$$

Where (I_{corr}) is corrosion current density, (Ea) is the apparent activation energy, (R) is the gas constant (8.314 J mol^{-1} K^{-1}), (T) is temperature in K, (A) is the Arrhenius factor,(h) is the Plank's constant (6.626 x 10^{-34} J.s), (N) is the Avogadro's number (6.022 x 10^{23} mol^{-1}), (ΔH*) is the enthalpy of activation and (ΔS*) is the entropy of activation.

The plot of log I_{corr} against 1/ T presented a linear relation with a slope (-Ea / 2.303R) and the intercept of the extrapolated line log A. Figure 8. The events showed that the value of Ea for an inhibited solution is higher than that for the blank solution, suggesting that dissolution of carbon steel (C.S) is slow in the presence of inhibitor, Table 11.

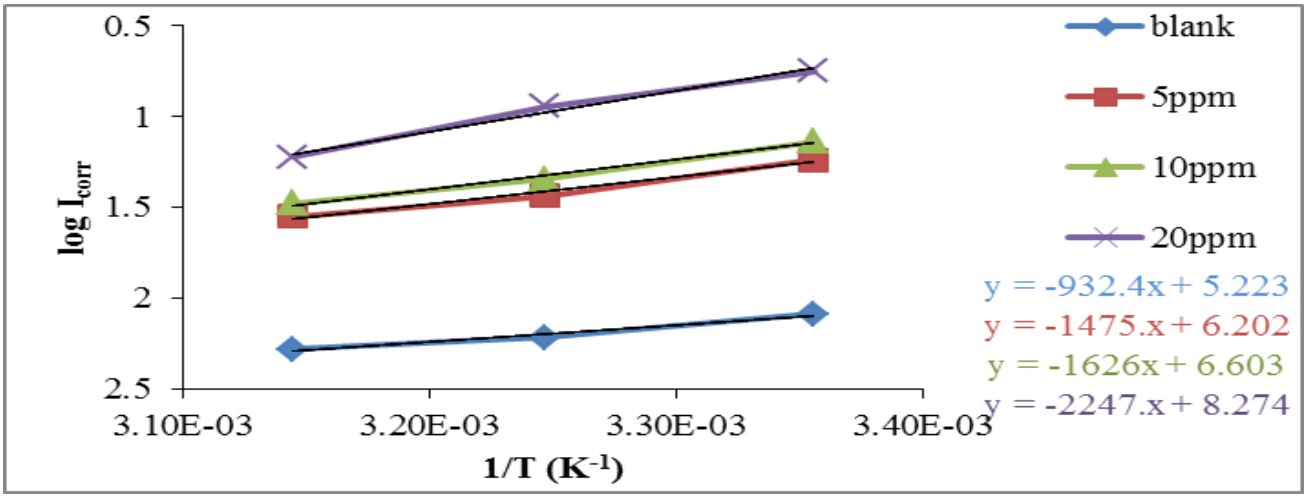

Figure 8: Plots of log I_{corr} vs (1/T) for the corrosion of carbon steel in 3.5% NaCl containing various concentrations of inhibitor

The enthalpy of activation ΔH* is obtained from the slope (ΔH*/ 2.303R) obtained from scheming (log I_{corr}/T) versus (1/T) with ΔS* which obtained from an intercept of [(log (R/ Nh) + (ΔS*/2.303R)], Figure 9. The positive sign of enthalpies ΔH* reflects the endothermic nature of dissolution process. The ΔH* for corrosion reaction increasing in the different concentration of compound **(4)**.The entropy of activation ΔS* in the blank and inhibitor has negative value, was changed when compound **(4)** was added at a temperature range (298-318 K) (Table 11), it indicates a decrease in entropy takes place ongoing from blank to the inhibitor [23]. The activation free energy demonstrates that the corrosion reaction of C-steel is non-spontaneous and increase with increasing temperature, assume that corrosion reaction increase with increasing temperature.

Table 11: Corrosion kinetic parameters for carbon steel in 3.5% NaCl in the blank and presence of different concentrations of compound (4)

Conc. (ppm)	ΔG kJ/ mol			ΔH* kJ/ mol	ΔS* kJ/ mol . K	Ea kJ/ mol	A Molecule/ cm. s
	298K	308K	318K				
0	61.037	62.572	64.107	15.293	-0.154	17.853	1.006E+29
5	65.840	67.188	68.535	25.676	-0.135	28.242	9.5851E+29
10	66.443	67.714	68.985	28.568	-0.127	31.133	2.41322E+30
20	68.799	69.750	70.701	40.458	-0.095	43.024	1.13135E+32

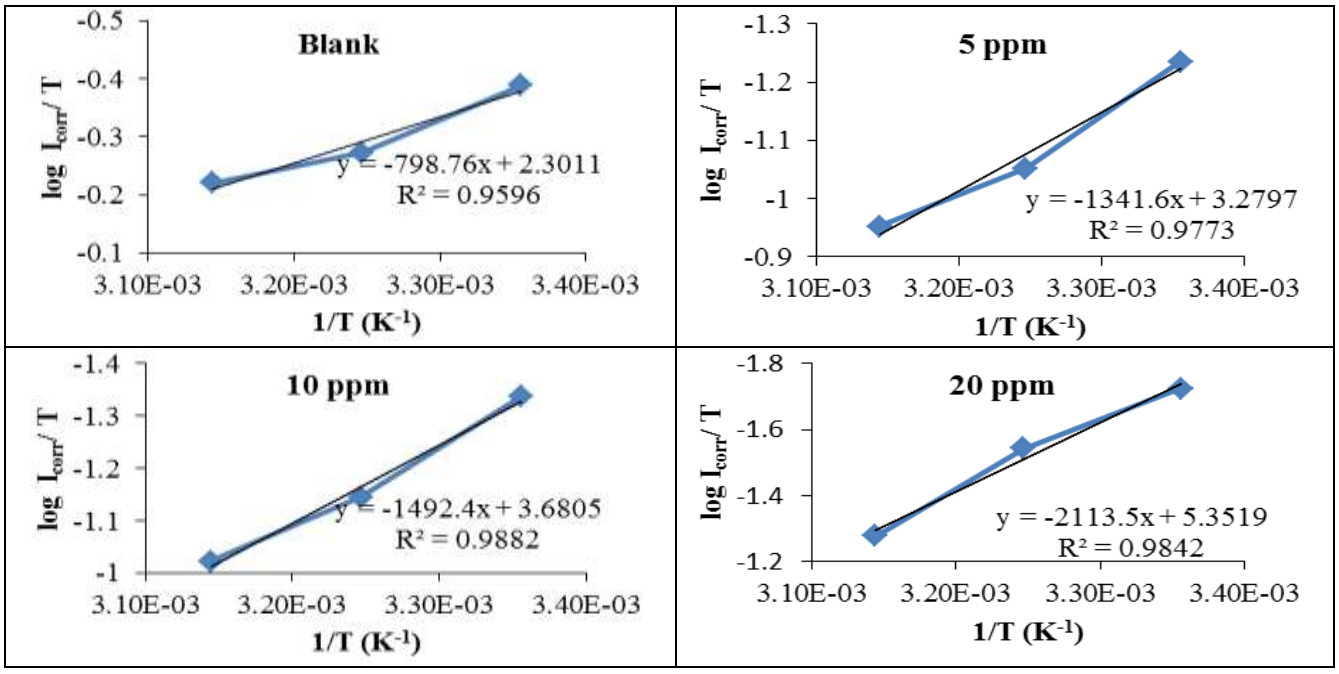

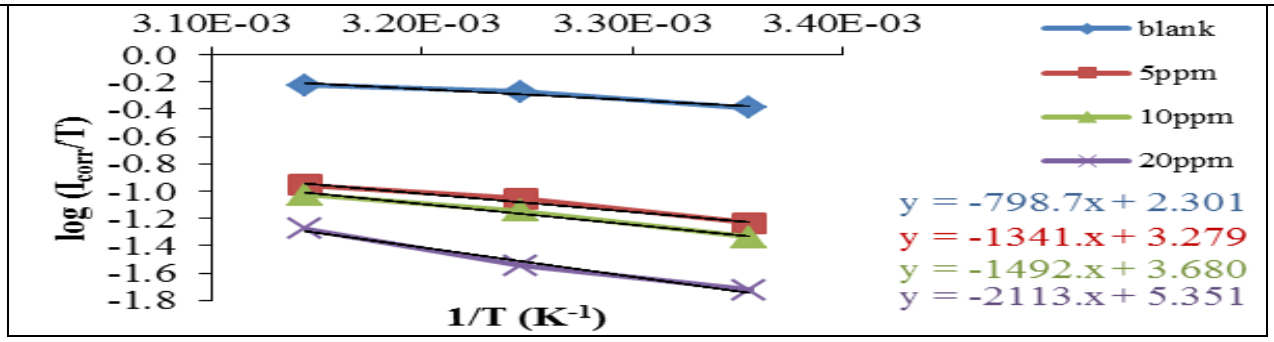

Figure 9: Arrhenius plots calculated from the corrosion current of C.S in 3.5% NaCl within blank and different concentrations of compound (4)

Conclusions

- Synthesis of novel 5-Nitroisatin derivatives (1-4) was found to be effective inhibitors for carbon steel corrosion in 3.5% NaCl solution.
- Quantum mechanical methods showed the compound (4) best inhibitor than others.
- The potentiodynamic polarisation measurements showed that the compound (4) can be classified as a mixed inhibitor in 3.5% NaCl solution.
- The adsorption of compound (4) on mild steel surface follows the Langmuir adsorption isotherm model.
- Isatin derivatives posses a wide range of biological activities, therefore, they used as a safety and nontoxic inhibitors.

References

1. M Pal, N Sharma, K Priyanka (2011) Synthetic and biological multiplicity of isatin: A Review, J. Adv. Sci. Res., 2(2):35-44.
2. G Mathur, S Nain (2014) Recent Advancement in Synthesis of Isatin as Anticonvulsant Agents: A Review, Med chem., 4 (4):417-427.
3. Z Hussain, E Yousif, A Ahmed, A Altaie (2014) Synthesis and characterization of Schiff's bases of sulfamethoxazole, Org.& Med. Chem. Letters, 4-1.
4. HM Abd El-Lateef, M Ismael, IM Mohamed (2015) Study of Some Bidentate Schiff Bases of Isatin as Corrosion Inhibitors for Mild Steel in Hydrochloric Acid Solution, Corros Rev, 33 (1-2):77-97.
5. RM Kubba, DA Challoob, SMH Al-Majidi (2017) PM3 and DFT quantum mechanical calculations of two new N benzyl-5-bromo isatin derivatives as corrosion inhibitors, Int. J. Sci.& Res., 6: 1656-1669.
6. S Chitra1, K Parameswari, A Selvaraj (2010) Dianiline Schiff Bases as Inhibitors of Mild Steel Corrosion in Acid Media, Int. J. Electro chem. Sci., 5: 1675-1697.
7. RM Kubba, AS Alag, SMH Al-Majidi (2017) Effect of Schiff's Bases as Corrosion Inhibitors on Mild Steel in Sulphuric Acid, Int. J. Sci. & Nat., 8 (3): 591-603.
8. SMH Al-Majidi, L Hamma (2015) Synthesis and antimicrobial evaluation activity of some new substituted spiro-thiazolidine, Imidazolinone and azetidine derivatives of 5-Bromo Isatin, J. Zank. Sula., 17 (1): 49-59.
9. SMH Al-Majidi, R Abdul-Hussein (2015) Synthesis and evaluation antimicrobial activity of some new S-substituted Quinazolinone containing pentagonal, hexagonal heterocyclic ring, J. Zank. Sula., 17 (1): 33-48.
10. A Becke (1993) Density-functional thermo chemistry. III. The role of exact exchange, J. Chem. Phys., 98: 5648-5652.
11. M Frisch, W Trucks, G Schlege, H Scuseria, G Robb, M Cheeseman, J Montgomery, J Vreven, T Kudin, K Burant, J Millam, J Iyengar, S Tomasi, J Barone, V Mennucci, B Cossi, M Scalmani, G Rega, N Petersson, G Nakatsuji, H Hada, M Ehara, M Toyota, K Fukuda, R Hasegawa, J Ishida, M Nakajima, T Honda, Y Kitao, O Nakai, H Klene, M Li, X Knox, J Hratchian, H Cross, J Bakken, V Adamo, C Jaramillo, J Gomperts, R Stratmann, R Yazyev, O Austin, A Cammi, R Pomelli, C Ochterski, J Ayala, P Morokuma, K Voth, G Salvador, P Dannenberg, J Zakrzewski, V Dapprich, S Daniels, A Strain, M Farkas, O Malick, D Rabuck, A Raghavachari, K Foresman, J

Ortiz, J Cui, Q Baboul, A Clifford, S Cioslowski, J Stefanov, B Liu, G Liashenko, A Piskorz, P Komaromi, I Martin, R Fox, D Keith, T Al-Laham, M Peng, C Nanayakkara, A Challacombe, M Gill, P Johnson, B Chen, W Wong, M Gonzalez C Pople JA (2009) Gaussian 03, Gaussian. Inc. Pittsburgh PA.

12. RM Kubba, AS Alag (2017) Schiff bases as corrosion inhibitor for aluminium in HCl solution, Int. J. Sci. & Res., 6 (6): 1632-1643.
13. S Safak, B Duran, A Yurt, G Turkoglu (2012) Corros. Sci., 54: 251-259.
14. RM Kubba, DA Challoob (2017) Int. J. Sci. & Nat., 8 (3): 1-18.
15. S Wolynec (2003) Técnicas Eletroquímicas em Corrosão, Editora da Universidade de São Paulo, São Paulo.
16. H Flitt, D Schweinsberg (2005) Evaluation of corrosion rate from polarization curves not exhibiting a Tafel region, Corros. Sci., 47: 3034-3052.
17. M Amin, S Rehim, H Abdel-Fatah (2009) Electrochemical frequency modulation and inductively coupled plasma atomic emission spectroscopy methods for monitoring corrosion rates and inhibition of low alloy steel corrosion in HCl solutions and a test for validity of the Tafel extrapolation method, Corros. Sci., 51: 882-894.
18. O Abiola (2006) Adsorption of 3-(4-amino-2-methyl-5pyrimidyl methyl)-4-methyl thiazolium chloride on mild steel, Corros. Sci., 48: 3078-90.
19. J Cruz, R Martinez, J Genesca, E Ochoa (2004) Experimental and theoretical study of 1-(2-ethylamino)2-methylimidazoline as an inhibitor of carbon steel corrosion in acid media, J. Electroan. Chem., 566 (1): 111-121.
20. M Bahrami, S Hosseini, P Pilvar (2010) Experimental and theoretical investigation of organic compounds as inhibitors for mild steel corrosion in sulfuric acid medium, Corros. Sci., 52: 2793-2803.
21. W Durnie, R DeMarco, A Jefferson, B Kinsella (1999) Development of a structure-activity relationship for oil field corrosion inhibitors, J. Electrochem. Soc., 146 (5): 1751-1756.
22. M Solomon, S Umoren, I Udosoro, A Udoh (2010) Inhibitive and adsorption behaviour of carboxymethyl cellulose on mild steel corrosion in sulphuric acid solution, Corros. Sci., 52 (4): 1317-1325.
23. N Soltani, M Behpour, S Ghoreishi, H Naeimi (2010) Corrosion inhibition of mild steel in hydrochloric acid solution by double Schiff bases, Corros. Sci., 52 (4): 1351-1361.

